BRITISH JOURNAL OF HOSPITAL MEDICINE

CASE REPORT

Imaging findings of breast leukaemia: a case series

Dandan Li[1]
Yuwei Xin[1]
Jiaan Zhu[1]
Author details can be found at the end of this article
Correspondence to:
Jiaan Zhu; Zhujiaan@pkuph.edu.cn

Abstract

Aims/Background Breast leukaemia (BL) is a rare breast malignancy that is treated differently from other malignant conditions. However, it is easily confused with other conditions; therefore, how to accurately diagnose is crucial. We retrospectively analysed the imaging findings of 13 patients to provide a diagnostic reference.

Methods From January 2015 to April 2023, 13 patients with BL confirmed by biopsy who underwent imaging in Peking University People's hospital were retrospectively analysed. The imaging findings obtained via ultrasound (US), mammography (MMG), magnetic resonance imaging (MRI), and positron emission tomography/computed tomography (PET/CT) were analysed, and the detection rates of these methods for diagnosing BL were compared.

Results Twenty-nine lesions were detected in the 13 patients. These patients presented with palpable masses or breast swelling several months after treatment for leukaemia, mainly involving the bilateral breasts. Ultrasonography was performed for 13 patients, and all lesions were detected. Most of the identified masses were hypoechoic and had indistinct boundaries, irregular shapes, no enhancement of the posterior echo, and no abundant blood flow. MMG was performed for five patients, revealing breast masses, architectural distortion, and no abnormalities. MRI was performed for four patients, and all lesions were detected; most of the lesions were hypointense on T1-weighted imaging and hyperintense on T2-weighted imaging and diffusion-weighted imaging, with a decreased apparent diffusion coefficient and inhomogeneous enhancement. The enhancement curves were mostly inflow patterns. PET/CT was performed for four patients; two patients had hypermetabolism, and the other two had no obvious radioactive uptake.

Conclusion Compared to MMG and PET/CT, US and MRI have higher detection rates. Furthermore, compared to MRI, US is inexpensive, convenient and efficient; therefore, it should be the first choice for diagnosing BL.

Key words: Breast leukaemia; Case report; Imaging findings

Submitted: 18 March 2024; Revised: 19 April 2024; Accepted: 30 April 2024

Introduction

Breast leukaemia (BL) is a rare breast malignancy that accounts for approximately 0.25% of all breast tumours (Khoury et al, 2000); however, the current description of BL can be found only in case reports. BL is mainly observed in patients with acute myeloid leukaemia and can occur at any age, ranging from 1 to 80 years (Glazebrook et al, 2014; Sung et al, 2023). It often presents as a palpable mass in the breast or breast swelling. BL is caused mainly by extramedullary recurrence of leukaemia, but its specific pathogenesis remains unclear. It may be related to residual microinfiltrating leukaemia lesions, which seed and propagate in the breast, leading to recurrence (Karbasian-Esfahani et al, 2008; Chen et al, 2010; Hussain et al, 2022); it may also be related to the abnormal expression of adhesion molecules, the immune phenotype on the cell surface, leukaemia subtypes, or the transformation of tumour cells in the breast microenvironment (Karbasian-Esfahani et al, 2008; Liu et al, 2016; Mosalem et al, 2020). BL is easily confused with other breast malignancies that are treated with endocrine therapy or mastectomy (Waks and Winer, 2019). However, unlike for other conditions, there is currently no clear expert consensus on the treatment of BL. Previous studies have used chemotherapy, local radiotherapy, secondary

How to cite this article:
Li D, Xin Y, Zhu J. Imaging findings of breast leukaemia: a case series. Br J Hosp Med. 2024. https://doi.org/10.12968/hmed.2024.0101

transplantation, or a treatment combined with novel targeted therapy (Karbasian-Esfahani et al, 2008; Houghtelin et al, 2015; Liu et al, 2016; DiNardo et al, 2023; Shatilova et al, 2021; De Cap et al, 2023; Cunningham, 2006). For BL, if only the discovered lesions or the whole affected breast are resected, other microinvasive lesions within the breast may be missed, leading to postoperative recurrence and ultimately requiring a second operation. Moreover, surgical removal of the breast has permanent physical and psychological effects on patients, significantly reducing their quality of life. Therefore, the accurate identification and diagnosis of BL are highly important. Although the final diagnosis requires histopathology, familiarity with the imaging characteristics of BL can help to establish an accurate diagnosis (Sosa et al, 2022). In this study, the imaging findings of 13 patients with BL were retrospectively analysed to provide a reference for the diagnosis of this disease.

Methods

Patient population

We enrolled 13 patients diagnosed with BL by pathological biopsy who underwent imaging at Peking University People's Hospital from January 2015 to April 2023. Patients who underwent imaging examinations in other hospitals were excluded since we were unable to obtain the images. In total, 29 lesions were identified. Among the included patients, 13 patients underwent ultrasound (US), five patients underwent mammography (MMG), four patients underwent magnetic resonance imaging (MRI), and four patients underwent positron emission tomography/computed tomography (PET/CT). The study was approved by the Ethics Committee of Peking University People’s hospital (No. 2018PHB179-01) and was performed in compliance with the Declaration of Helsinki. Written informed consent was obtained from all patients.

Imaging

Mammography

Mammography was performed using a Digital MMG machine (GE Healthcare, Milwaukee, Wisconsin). Standard craniocaudal and mediolateral oblique views were obtained, with additional views if necessary. We reviewed the following features: (1) Breast Imaging Reporting and Data System (BI-RADS) (Spak et al, 2017) classification of the breast parenchyma; (2) density, shape, and boundary of the breast mass; and (3) other associated symptoms (oedema and thickening of the breast skin, inverted nipples, and swelling of the axillary lymph nodes).

Ultrasound

The US instruments used in the study comprised Siemens S3000 (Siemens, Munich, Germany), Logic E9 system (GE Healthcare, Chicago, IL, USA), IU 22 scanner (Philips, Amsterdam, Netherlands), and Mindray DC-8 (Mindray, Shenzhen, China), with high-frequency transducers. We reviewed the following features: (1) lesion position (left, right, or bilateral breast), number (single or multiple), size, composition (cystic or solid), shape (regular or irregular), margin (distinct or indistinct), internal echo (hyperecho, hypoecho, equal echo, or mixed echo), and posterior acoustic enhancement (presence or absence); (2) blood flow (Grade 0, no blood flow; Grade I, a small amount of dot-like blood flow; Grade II, one longer blood flow through the mass or three dot-like blood flows) (Nasief et al, 2019); (3) BI-RADS grade of the lesions determined according to the American College of Radiology (ACR) classification system (Spak et al, 2017); and (4) axillary lymph node involvement (with or without).

Magnetic resonance imaging

We used a 3.0T MRI system scanner (Discovery 750W, GE Healthcare, Chicago, IL, USA) equipped with an 8-channel breast-dedicated coil. The patients were placed in a prone position with natural sagging of both breasts, and scanning of the bilateral breast and axillary regions was performed. MRI was performed in both the axial and sagittal planes. The breast MRI sequences and scanning order were as follows: (1) axial T2-weighted (T2W) fat-suppressed imaging with a short time inversion recovery (STIR) sequence with the following parameters: repetition time (TR), 3848 ms; echo time (TE), 83 ms; slice thickness, 6.0 mm; slice gap, 1.5 mm; field of view (FOV), 350 mm×350 mm; and matrix, 320×256; (2) diffusion-weighted imaging (DWI) with an echo planar imaging sequence with the following parameters: TR, 3120 ms; TE, 76 ms; slice thickness, 4.0 mm; slice gap, 1.0 mm; FOV, 350 mm×350 mm; matrix, 128×128; and diffusion-sensitive coefficient (b-value), 800 s/mm^2; and (3) dynamic contrast-enhanced imaging with a gradient echo sequence, consisting of an axial T1-weighted fat-suppressed sequence with the following parameters: TR, 4.5 ms; TE, 2.1 ms; slice thickness, 1.5 mm; no gap; FOV, 350 mm×350 mm; and matrix, 384×320. After the axial scan, 15 mL of gadopentetate dimeglumine (Magnevist, Bayer HealthCare Pharmaceuticals, Leverkusen, Germany) was injected, at a dose of 0.1 mmol/kg, at a flow rate of 3 mL/s, followed by 20 mL of saline. Twenty-three seconds after the injection, a continuous scan was performed six times, with each scan lasting approximately 60 s, for a total scan time of 6 min 23 s. We reviewed the following characteristics: (1) the presence or absence of a lesion in the breast; (2) lesion shape (circular, lobulated, or irregular), boundary (distinct or indistinct), T1-weighted imaging (T1WI) signal (hyperintensity, hypointensity, or isointensity), T2-weighted imaging (T2WI) signal (hyperintensity, hypointensity, or isointensity), and DWI signal (hyperintensity, hypointensity, or isointensity); (3) lesion enhancement and type of enhancement curve (inflow, outflow, or plateau pattern); (4) BI-RADS grade (Spak et al, 2017).

Positron emission tomography/computed tomography

Positron emission tomography/computed tomography was performed using a GE Discovery PET/CT VCT. All patients fasted for at least 6 h before examination, and their blood glucose level was confirmed to be less than 8 mmol/L. ^{18}F-Fluorodeoxyglucose (^{18}F-FDG) was injected intravenously at a dose of 5.55 MBq/kg. Approximately 50 min later, images were acquired from the base of the skull to the sole. PET images were reconstructed using ordered subset expectation maximisation, and the reconstruction parameters were 28 subsets and two iterations. Three-dimensional PET, CT, and their fusion images were reconstructed using computer processing. FDG uptake was considered abnormal when the uptake in the tumour area was significantly greater than that in the background. After correcting for radioactive decay, the maximum standardised uptake value (SUV_{max}) of FDG was semi-quantitatively analysed using the formula SUV=ROI/ID/BW, where SUV is the SUV_{max}, ROI is the average region of interest activity (in millicuries per milliliter), ID is the injection dose (in millicuries), and BW is the body weight (in grams). We reviewed (1) the presence or absence of lesions with a high metabolism and (2) the SUV of the lesions.

Results

Patients and clinical signs

A total of 13 patients were enrolled, including 12 (92.31%) females and 1 (7.69%) male. The patients' ages ranged from 17 to 63 years, with an average age of 35 (34.92±13.79) years. Among them, 11 patients (84.62%) presented with palpable masses in the breast, and the sizes of these masses ranged from 0.8 cm to 9.2 cm, with an average of 3.64 (3.64±2.05) cm. The other two patients (15.38%) presented with bilateral breast swelling. All 13 patients developed symptoms after leukaemia treatment; 10 patients (76.92%) developed symptoms 3–22 months after haematopoietic stem cell transplantation (HSCT), with an average of 13 months, and three patients (23.08%) developed symptoms 1–44 months after leukaemia chemotherapy, with an average of 19 months. Among the 13 patients, 8 (61.54%) experienced isolated breast recurrence, whereas the other 5 (38.46%) experienced recurrence not only in the breast (Figure 1A) but also in other parts of the body (Table 1), including the chest wall (Figures 1B, C), retroperitoneum (Figures 1D–F), orbit (Figures 2A–D), eyelid, and skin. In addition, seven patients (53.85%) simultaneously developed graft-vs-host disease (GVHD), involving the intestines, skin, and liver. Four patients (30.77%) had axillary lymph

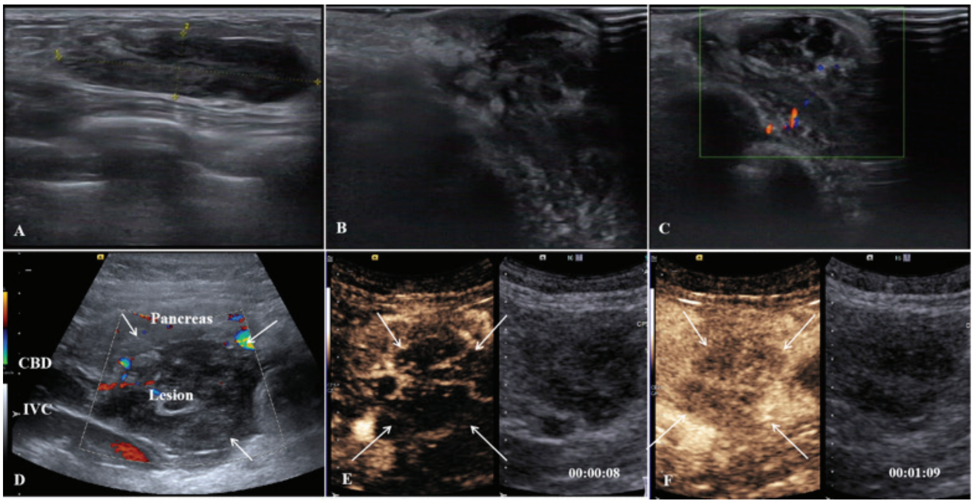

Figure 1. A 27-year-old woman presented with multiple extramedullary recurrences after haematopoietic stem cell transplantation (HSCT). (A) After 18 months of HSCT, the patient's left breast presented with a mass. (B,C) The patient's whole left breast was resected; 4 months later, the patient's left chest wall exhibited a mass again with abundant blood flow. (D) Twenty-two months later, a retroperitoneal mass appeared (as indicated by the arrows). It was located behind the head of the pancreas and compressed the common bile duct, resulting in obstruction. (E,F) Contrast-enhanced ultrasound (US) showed prominent enhancement in the arterial phase, and the agent quickly washed out (as indicated by the arrows).

Table 1. Clinical characteristics of 13 patients

Case	Sex	Age	Side	Clinical feature	ALP	Therapy	Recurrence time[1] (months)	Extramedullary recurrence (except breast)	GVHD	Pathologic type
1	F	33	bilateral	breast swelling	+	chemotherapy	1			MS
2	F	27	bilateral	mass	–	HSCT	18	chest wall, retroperitoneum		B-LBL
3	F	30	left	mass	–	HSCT	8			B-LBL
4	M	24	bilateral	mass	+	HSCT	15		intestine, skin	T-LBL
5	F	46	left	mass	–	HSCT	3.5		liver, skin	MS
6	F	20	bilateral	mass	+	chemotherapy	12			B-LBL
7	F	17	bilateral	breast swelling	+	chemotherapy	44			B-LBL
8	F	24	bilateral	mass	–	HSCT	22		intestine	MS
9	F	41	bilateral	mass	–	HSCT	20	bilateral eyelids	liver	MS
10	F	52	left	mass	–	HSCT	5		skin	MS
11	F	63	bilateral	mass	–	HSCT	12	skin	liver	T-LBL
12	F	47	right	mass	–	HSCT	9	periorbital	liver, intestine	MS
13	F	30	bilateral	mass	–	HSCT	18			MS

Abbreviations: F, female; M, male; ALP, axillary lymphadenopathy; HSCT, haematopoietic stem cell transplantation; GVHD, graft-vs-host disease; MS, myeloid sarcoma; B-LBL, B-lymphoblastic lymphoma/leukaemia; T-LBL, T-lymphoblastic lymphoma/leukaemia.

'+', axillary lymphadenopathy; '–', no axillary lymphadenopathy. '1', time to recurrence after treatment for leukaemia.

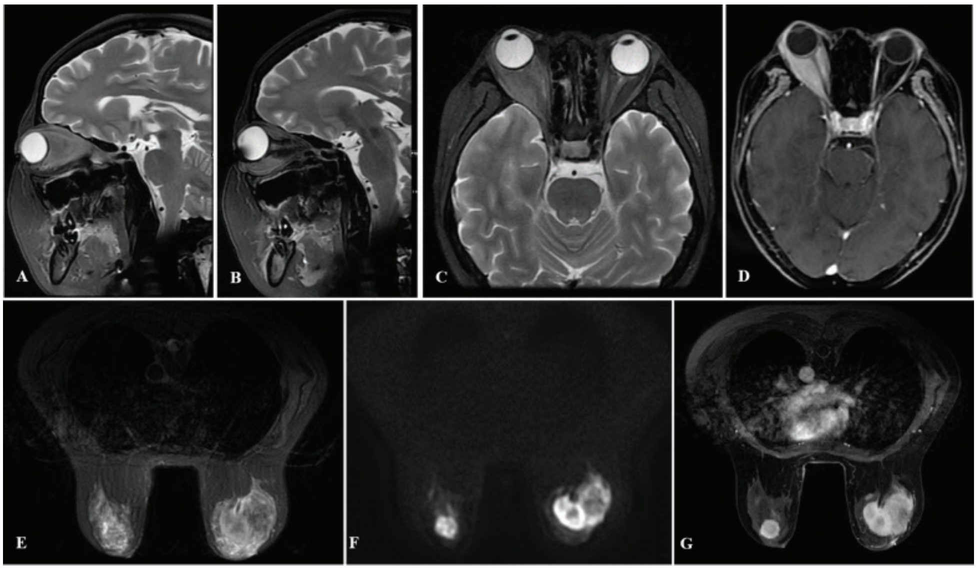

Figure 2. A 41-year-old woman presented with a soft tissue mass in the bilateral orbits and breasts 20 months after HSCT. All right extraocular muscles, left superior and inferior rectus muscles, and right optic nerve were involved. The lesions exhibited hyperintensity on T2 STIR images in the sagittal (A,B) and axial (C) views and homogeneous enhancement on T1WI (D). The bilateral breast masses also exhibited hyperintensity on T2 STIR (E) and DWI (F) images and homogeneous enhancement on T1WI (G). STIR, short time inversion recovery; T1WI, T1-weighted imaging; DWI, diffusion-weighted imaging.

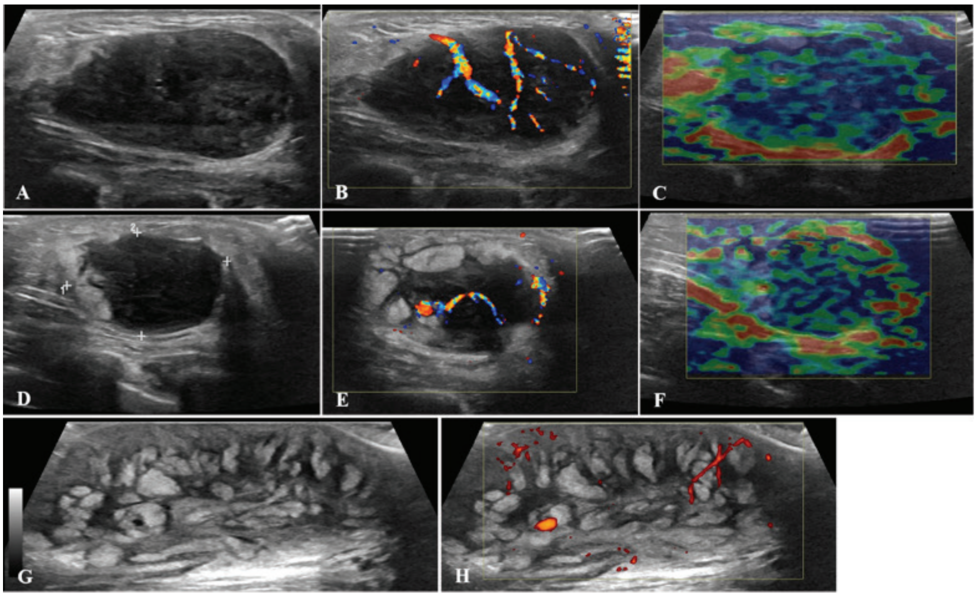

Figure 3. Ultrasound images of a 27-year-old woman 18 months after HSCT. The pathological diagnosis was B-lymphoblastic lymphoma/leukaemia. (A–C) There was a hypoechoic mass in the lateral upper quadrant of the left breast, with a well-defined boundary, regular shape, lack of enhancement of posterior echo and abundant blood flow; the elasticity score was 4 points. (D–F) Another hypoechoic mass in the margin of the left breast, with a well-defined boundary, regular shape, and oedema of the peripheral tissue; the elastic score was also 4 points. (G,H) The soft tissue of the axillary region presented with oedema and thickening as well as abundant blood flow.

node enlargement and one patient had edema of axillary soft tissue *(***Figures 3G,H***)*. The pathologic types included myeloid sarcoma (53.85%), B-cell lymphoblastic lymphoma/leukaemia (30.77%), and T-cell lymphoblastic lymphoma/leukaemia (15.38%) (**Table 1**).

Ultrasound

Thirteen patients underwent US examination; nine (69.23%) presented with bilateral breast lesions, whereas the other four patients (30.77%) presented with unilateral breast lesions. Eleven patients (84.62%) presented with breast masses, for a total of 29 masses; the other 2 (15.38%) presented with a distorted structure (Figure 4A). The mass characteristics are listed in Table 2. Most of the masses had irregular shapes (68.97%); indistinct boundaries (55.17%); hypoechoic lesions (96.55%) (Figures 3A,D); no enhancement of the posterior echo (79.31%); and no abundant blood flow (58.62%), which was visualised as point or short strip blood flow (grade 0–2), while a few masses had abundant blood flow (Figures 3B,E). Three patients underwent elastography, and their scores were 3, 3 and 4, respectively (Figures 3C,F).

Table 2. Ultrasound findings in 29 tumours

Characteristic	No. of findings
Shape	
Regular	9 (31.03%)
Irregular	20 (68.97%)
Margin	
Distinct	13 (44.83%)
Indistinct	16 (55.17%)
Echo pattern	
Hypoechoic	28 (96.55%)
Mixed	1 (3.45%)
Posterior enhancement	
Enhancement	5 (17.24%)
No enhancement	23 (79.31%)
Attenuation	1 (3.45%)
Colour Doppler grading	
0	4 (13.79%)
1	10 (34.48%)
2	3 (10.35%)
3	8 (27.59%)
No grading	4 (13.79%)
BI-RADS	
3	1 (3.45%)
4a	5 (17.24%)
4b	2 (6.90%)
4c	1 (3.45%)
5	4 (13.79%)
No grading	16 (55.17%)

BI-RADS,Breast Imaging Reporting and Data System.

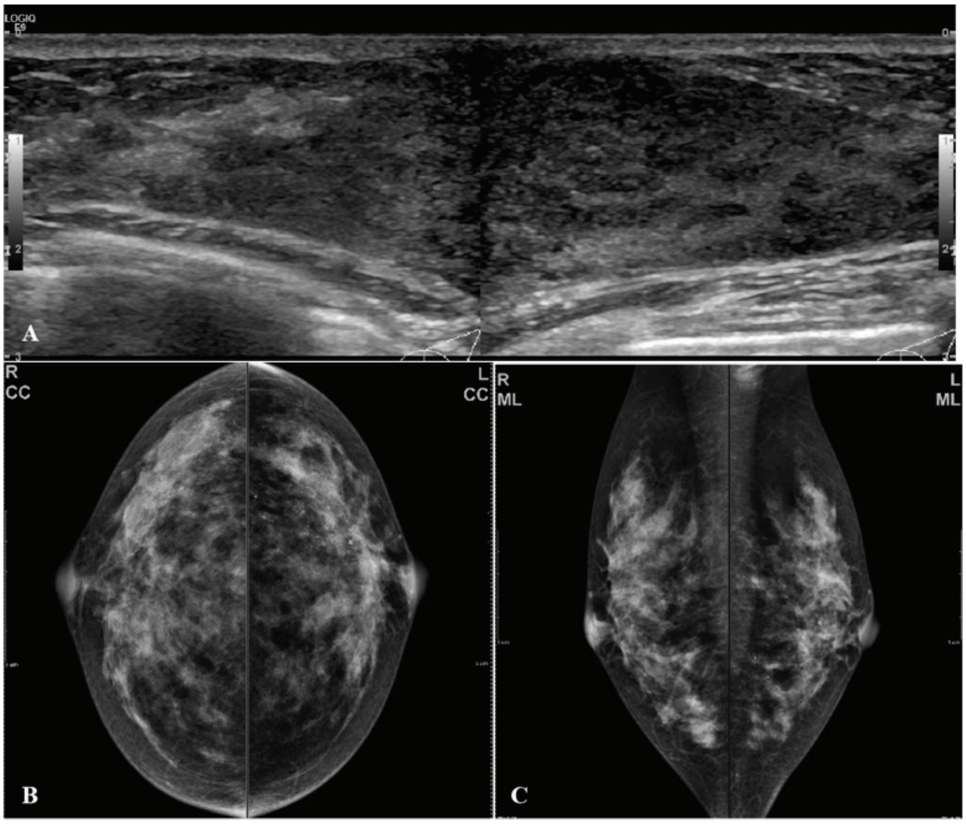

Figure 4. A 20-year-old woman presented with bilateral masses in the breast 12 months after chemotherapy. A core needle biopsy confirmed B-lymphoblastic lymphoma/leukaemia. (A) Distortion of the parenchymal structure of both breasts. (B,C) MMG showed no abnormalities in either breast.

Mammography

Five patients underwent MMG, and their breast parenchymal density was graded as BI-RADS 3 (60.00%) or BI-RADS 4 (40.00%). Among the patients whose breast parenchymal density was graded BI-RADS 3, two patients presented with visible masses (seven masses in total), and the other patient presented only locally heterogeneous density, not a mass. The characteristics of seven masses are presented in Table 3. The other 2 patients with a breast parenchymal density graded as BI-RADS 4 had no abnormalities on MMG (Figures 4B,C).

Magnetic resonance imaging

Four patients underwent MRI, and 14 lesions were detected. Consistent with the findings of previous studies (Shin, 2016), most of the lesions were slightly hypointense (92.86%) on T1WI and slightly hyperintense (85.71%) on T2WI (Figures 2E and 5A–C). DWI showed obvious hyperintensity (Figures 2F and 5D), and the apparent diffusion coefficient (ADC) decreased. The lesions all exhibited significant enhancement, and the enhancement curves were mostly inflow patterns (42.86%) (Figures 2G and 5E,F) (Table 4).

Positron emission tomography/computed tomography

Positron emission tomography/computed tomography was performed for four patients, and nine lesions were detected. Six lesions (66.67%) showed intense hypermetabolism (Figures 6C–E), which were all detected on Ultrasound (Figures 6A,B). The SUV_{max} ranged from 4.3 to 4.9, with an average of 4.4. The other three (33.33%) lesions did not show obvious uptake of the agent.

Table 3. Mammography findings in 7 masses

Characteristic	No. of findings
Shape	
Regular	1 (14.29%)
Irregular	6 (85.71%)
Margin	
Distinct	1 (14.29%)
Indistinct	6 (85.71%)
Density	
High	7 (100%)
Calcification	
With	1 (14.29%)
Without	6 (85.71%)

Table 4. Magnetic resonance imaging findings in 14 tumours

Characteristic	No. of findings
Shape	
Round	1 (7.14%)
Lobular	2 (14.29%)
Irregular	11 (78.57%)
Margin	
Distinct	7 (50.00%)
Indistinct	7 (50.00%)
T1WI	
Slight hypointensity	13 (92.86%)
Heterogeneous hypointensity	1 (7.14%)
T2WI	
Slight hyperintensity	12 (85.71%)
Slight hypointensity	2 (14.29%)
DWI	
Hyperintensity	14 (100%)
ADC	
Hypointensity	14 (100%)
Enhancement	
Significant enhancement	14 (100%)
Enhancement curve	
Inflow	6 (42.86%)
Platform	5 (35.71%)
Outflow	3 (21.43%)

T2WI,T2-weighted imaging; DWI, diffusion-weighted imaging; ADC, apparent diffusion coefficient.

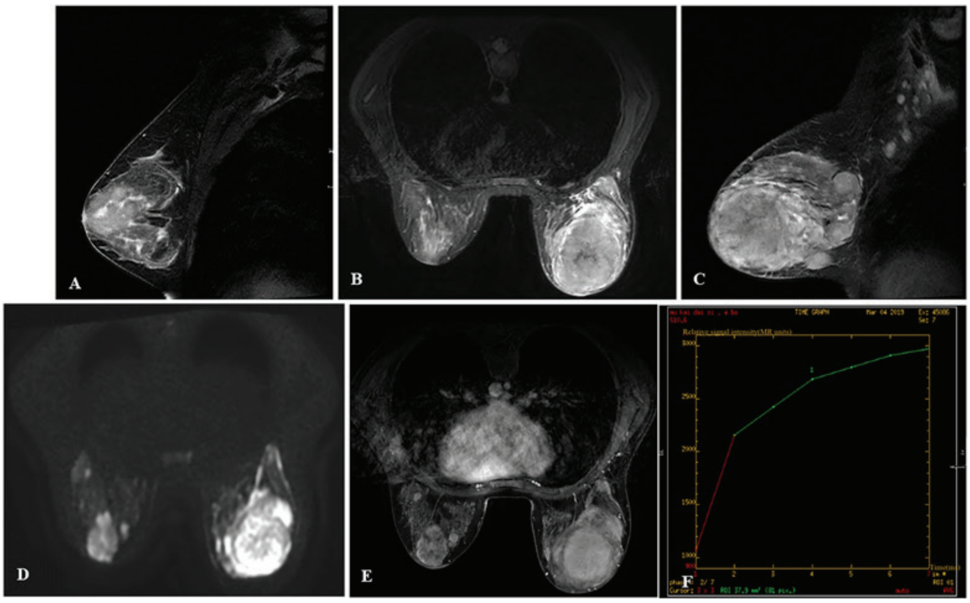

Figure 5. Magnetic resonance imaging image of a 17-year-old woman with bilateral breast swelling after 44 months of chemotherapy. Pathology revealed B-lymphoblastic lymphoma/leukaemia. (A–C) The lesions showed hyperintensity in T2WI-STIR images, and the mass in the right breast almost completely replaced the entire breast tissue. (D) The lesions showed hyperintensity on DWI. (E) Contrast-enhanced T1WI showing heterogeneous enhancement. (F) Kinetic analysis obtained from foci within the mass demonstrated rapid enhancement.

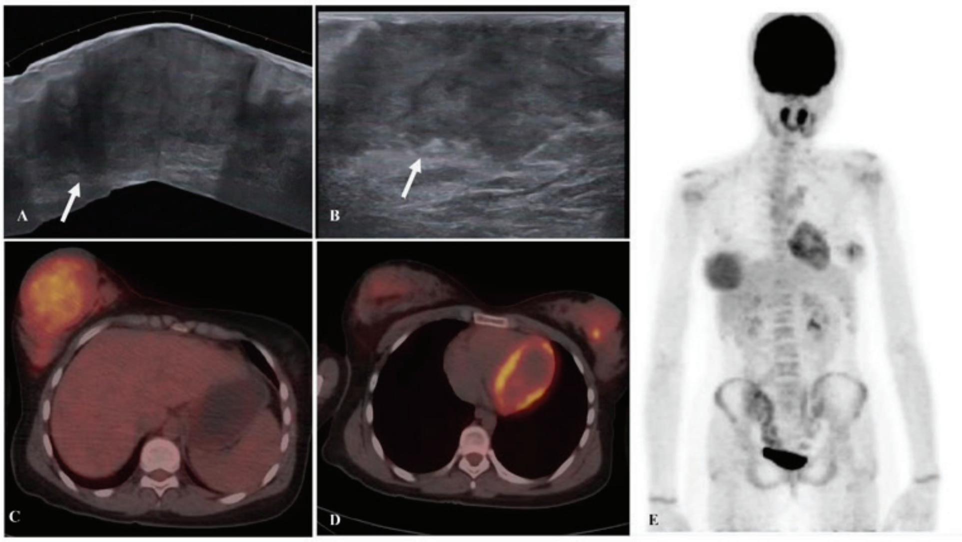

Figure 6. Ultrasound and positron emission tomography/computed tomography (PET/CT) images of a 17-year-old woman with bilateral breast swelling after 44 months of chemotherapy. Pathologic analysis revealed B-lymphoblastic lymphoma/leukaemia. US revealed a hypoechoic mass (as indicated by the arrows) in the right (A) and left (B) breasts, and (C,D) PET/CT showed intense hypermetabolism. (E) The maximal intensity projection of PET/CT showed elevated metabolism in both breasts.

Comparison among ultrasound, mammography, magnetic resonance imaging and positron emission tomography/computed tomography

In patients who underwent US and MRI, all the lesions were detected, for a detection rate of 100%, and no false negatives were observed. Among the 5 patients who underwent MMG, two (40.00%) had no significant abnormalities, with a breast parenchymal density grade of BI-RADS 4; however, their US examination all revealed abnormalities, suggesting that the MMG results included false negatives. Similarly, among the four patients who underwent PET/CT, two (50%) patients did not have hypermetabolic lesions, whereas on US or MRI, all the lesions were detected, suggesting that PET/CT also exhibited false-negative results (Table 5).

Follow-up

We obtained US images of four patients after treatment (Table 5); in two of them, the lesions were significantly reduced. Unfortunately, over time (5 months and 10 months), two patients relapsed again (Figures 7A–F).

Discussion

Breast leukaemia can occur at any age ranging from 1 to 80 years, with a median age of 33 years (Kumar et al, 2010; Glazebrook et al, 2014). In our study, the ages ranged from 17 to 63 years, with an average age of 35 (34.92±13.79) years. BL usually occurs after treatment for leukaemia, and this was the case for all of the patients in our study (Surov et al, 2012; Surov, 2013). The most common pathological type of tumour was myeloid sarcoma (MS), which is consistent with the findings of previous studies (Surov et al, 2012; Ge et al, 2014; Glazebrook et al, 2014). BL usually occurs in bilateral breast, which is different from breast cancer (Yang et al, 2007; Waks and Winer, 2019). This difference may be related to the residual microinvasive lesions in the breasts during leukaemia. According to previous case reports, almost all patients were female, and only one male patient was reported (Chim et al, 2000). In our study, we also included a male who presented with a palpable breast mass 15 months after HSCT but was misdiagnosed with gynaecomastia; this was later confirmed as BL by biopsy. After chemotherapy, the lesions disappeared; however, 5 months later, the lesions relapsed. The possible reason for the relapse may be residual microinvasion of the breasts.

In addition, seven patients developed GVHD; theoretically, GVHD has an antileukemia effect and can prevent the relapse of leukaemia to some extent (Goker et al, 2001; Lee et al, 2005; Karbasian-Esfahani et al, 2008). However, although the seven patients had

Table 5. Comparison of ultrasound, mammography, magnetic resonance imaging, and positron emission tomography/computed tomography and follow-up results

Case	Side	US	MMG	MRI	PET/CT
1	Bilateral	+[1]	+	+	
2	Bilateral	+			
3	Left	+			
4	Bilateral	+[1,2]			
5	Left	+	–		–
6	Bilateral	+	–		
7	Bilateral	+		+	+
8	Bilateral	+[1,2]			
9	Bilateral	+	+	+	
10	Left	+[1]	–		+
11	Bilateral	+			
12	Right	+			
13	Bilateral	+		+	–

Abbreviations: US, ultrasound; MMG, mammography; MRI, magnetic resonance imaging; PET/CT, positron emission tomography/computed tomography.

'+', positive findings; '–', no positive findings; '1', the lesions decreased in size or disappeared;

'2', the lesions relapsed after they disappeared.

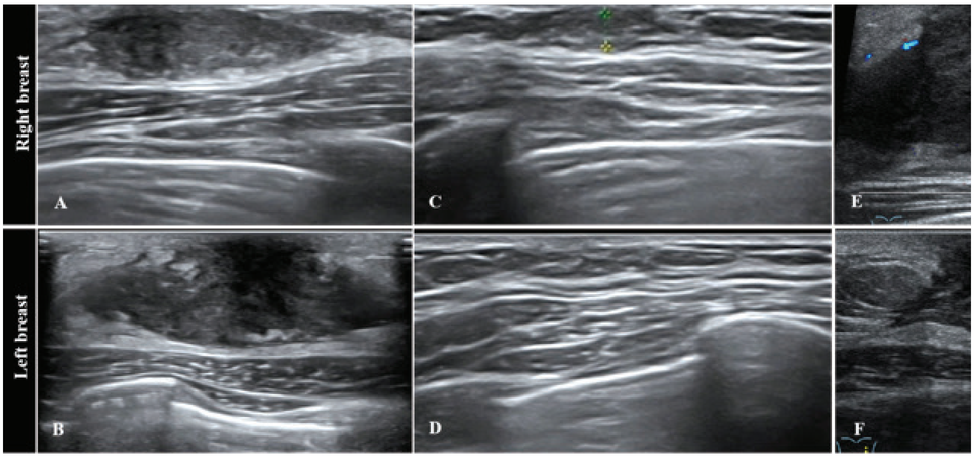

Figure 7. Changes in US images of a 24-year-old male after HSCT. (A,B) US image showed a hypoechoic mass on the deep side of both nipples, indicating male gynaecomastia. Biopsy confirmed T-lymphoblastic lymphoma/leukaemia. (C, D) After 3 months of chemotherapy, US showed that the lesions had obviously diminished. (E,F) However, 5 months later, the lesions relapsed.

GVHD, they still experienced leukaemia infiltration in the breast and multiple other extramedullary organs. A possible explanation is that GVHD is less effective at preventing extramedullary recurrence because of immune escape or the transformation effect of the breast microenvironment in leukaemia (Gaudichon et al, 2019; Cunningham, 2021); thus, microinvasive lesions in the breast or other organs may not be completely eliminated by GVHD, leading to recurrence after treatment (Galimberti et al, 2006; Pagliuca et al, 2023).

In our study, the most common US characteristic of BL was a mass, which was observed in 11 patients (85.00%). The masses were mainly hypoechoic (92.00%), irregularly shaped (77.00%), and had indistinct boundaries (62.00%) and no enhancement of the posterior echo (77.00%), which was consistent with the results of other reports (Surov et al, 2012; Glazebrook et al, 2014; Aslan and Pourbagher, 2017; Myers et al, 2022). It has been reported that blood flow in BL is abundant (Likaki-Karatza et al, 2002; Surov et al, 2012; Kulkarni et al, 2016; Sager et al, 2019; Kim and Kim, 2019); however, in our study, only a few masses (27%) had abundant blood flow (Grade 3), while the majority (57.00%) had poor blood flow (Grade 0–2). This difference may be related to the sensitivity of the equipment to blood flow or incorrect settings, such as setting the colour scale too high to indicate low-velocity blood flow. In addition, in our study, three patients underwent elastography, and their scores were 3, 3, and 4, respectively, indicating that the tumour was not hard, unlike those observed in breast cancer (Carlsen et al, 2015; Li et al, 2023). This difference might be related to the greater number of tumour cells and fewer fibrous components in the lesions (Abdulkadir et al, 2017; Aslan and Pourbagher, 2017; Lee et al, 2022). However, a low elasticity may affect radiologist judgment, leading to underestimation of the BI-RADS grade (Erduran et al, 1999; Zhang et al, 2020; Masood et al, 2021). Therefore, if malignant US features are found in the breasts of leukaemia patients but the elastography results are low, the possibility of BL should be considered.

In our study, there were three MMG patterns among the 5 patients: breast masses (40.00%), architectural distortion (20.00%), and no abnormalities (40.00%). Consistent with the findings of previous studies (Karbasian-Esfahani et al, 2008; Surov et al, 2012; Glazebrook et al, 2014), there were false negatives, possibly due to the high density of the background breast parenchyma, which resulted in the mass being obscured by the dense breast parenchyma and a missed diagnosis. The two patients in our study who presented with false negatives were graded as BI-RADS 4. However, our false-negative rate was greater than those of previous studies, possibly due to differences in breast density among different races. The breast parenchyma of most Chinese women is relatively dense and has little fat; while in most Western countries, women's breasts have more fat, so their density is lower, making it easier to detect masses and resulting in a lower false-negative rate. It can be inferred that for patients with dense breasts, combination of MMG with other methods is needed to reduce the number of missed diagnoses.

In our study, most patients with BL exhibited slight hypointensity (93.00%) on T1WI and slight hyperintensity (86.00%) on T2WI; DWI showed significant hyperintensity, and the ADC decreased, which is consistent with the findings of other studies (Koh and Collins, 2007; Surov et al, 2012; Aslan and Pourbagher, 2017; Sager et al, 2019; Durhan and Demirkazık, 2021; Ghosh et al, 2023; Kim, 2013; Basara and Orguc, 2012). The hyperintensity on DWI and reduced ADC indicate a high cellular composition and density within the tumour, which are characteristic of malignant tumours (Koh and Collins, 2007). A few studies have shown that the ADC of BL is lower than that of breast cancer (Durhan and Demirkazık, 2021). The lesions presented significant enhancement, with three types of enhancement patterns, inflow (42.86%), plateau (35.71%), and outflow (21.43%), which is consistent with the findings of other studies (Surov et al, 2012; Sager et al, 2019; Ghosh et al, 2023).

For patients who underwent ^{18}F-FDG PET/CT, most lesions (67.00%) were hypermetabolic, with an average SUV of 4.4, consistent with the results of other studies (Buck et al, 2004; Glazebrook et al, 2014; Myers et al, 2022). However, a few lesions (33.00%) showed no obvious FDG uptake, although all of these lesions presented as masses on US and were confirmed by biopsy. Thus, we can infer that both the PET/CT and MMG results included false negatives. The reason for these false negatives is not yet clear; it may be related to the diagnostic criteria used to distinguish benign and malignant lesions. If the uptake value of BL is lower than the established criterion, false-negative results may occur. In addition, this difference may also be related to the low resolution of the equipment, small lesion volume, pathological subtypes of BL, and levels of Ki-67(Buck et al, 2004). To reduce the false-negative rate of PET/CT, a comprehensive judgment should be made according to the clinical history, US, MRI, and other examinations when diagnosing patients. As a whole-body imaging technology, PET/CT has great advantages in disease staging and the evaluation of therapeutic effects (Liu et al, 2016).

Our study has several limitations: it was retrospective, the sample size was small, and not every patient underwent all the imaging examinations. In addition, we did not conduct follow-ups for all patients with every imaging examination; therefore, we did not summarise the general imaging changes after treatment. Methods to detect residual microinvasive lesions more effectively after treatment should be studied. These are promising avenues for future study.

Conclusion

This study is the largest series reporting BL to date, and includes more comprehensive imaging data than previous studies. We found that MMG and PET/CT yield false negatives; in comparison, US and MRI had higher detection rates. Therefore, even if no abnormal lesions are detected on MMG and PET/CT, other imaging methods or clinical history should be performed to make a comprehensive diagnosis of patients with suspected BL. We believe that US is the preferred imaging modality for detecting breast abnormalities in patients with BL; it offers a higher detection rate comparable to MRI, and is more convenient and inexpensive. Since BL is easily confused with other conditions, it is recommended that clinical history be taken into account for diagnosis; in other words, if the patient has leukaemia, we should highly suspect that the lesion in her breast is BL.

Learning points

- The imaging findings of breast leukaemia are nonspecific compared to other breast malignancies, thus incorporating medical history is crucial for accurate diagnosis.
- Ultrasound and MRI have a higher detection rate for breast leukaemia compared to mammography and PET/CT.
- Ultrasound is more accurate than mammography and PET/CT, and more cost-effective than MRI for diagnosing breast leukaemia, making it the preferred initial choice.
- Dense breasts can obscure lesions, posing a significant challenge for mammography.

Author details

[1]Department of Ultrasound, Peking University People's Hospital, Beijing, China

Abbreviations

BL, breast leukaemia; US, ultrasound; MMG, mammography; MRI, magnetic resonance imaging; PET/CT, positron emission tomography/computed tomography; T1WI, T1-weighted imaging; T2WI, T2-weighted imaging; STIR, short time inversion recovery; DWI, diffusion-weighted imaging; ADC, apparent diffusion coefficient; BI-RADS, Breast Imaging Reporting and Data System; TR, repetition time; TE, echo time; ^{18}F-FDG, ^{18}F-fluorodeoxyglucose; SUV, standardised uptake value; ROI, region of interest; ID, injection dose; BW, body weight; GVHD, graft-vs-host disease; MS, myeloid sarcoma; B-LBL, B-lymphoblastic lymphoma/leukaemia; T-LBL, T-lymphoblastic lymphoma/leukaemia.

Availability of data and materials

All data generated or analysed during this study are included in this article.

Author contributions

DDL, YWX and JAZ designed the research study. DDL performed the research. DDL drafted the manuscript. All authors contributed to important editorial changes in the manuscript. All authors read and approved the final manuscript. All authors have participated sufficiently in the work and agreed to be accountable for all aspects of the work.

Ethics approval and consent to participate

The study was approved by the Ethics Committee of Peking University People's hospital (No. 2018PHB179-01) and was performed in compliance with the Declaration of Helsinki. Written informed consent was obtained from all patients.

Acknowledgements

We are grateful to the patients for their collaboration.

Funding

This research received no external funding.

Conflict of interest

The authors declare no conflict of interest.

References

Abdulkadir E, Gulhan E, Ulus S. Differentiation of secondary involvement of the breast by lymphoreticular malignancy from fibroadenoma using ultrasound elastography: a report of two cases. Indian J Radiol Imaging. 2017;27(02):237–240. https://doi.org/10.4103/ijri.IJRI_238_16

Aslan H, Pourbagher A. Breast involvement by hematologic malignancies: ultrasound and elastography findings with clinical outcomes. J Clin Imaging Sci. 2017;7:42. https://doi.org/10.4103/jcis.JCIS_65_17

Basara I, Orguc S. Giant breast involvement in acute lymphoblastic leukemia: MRI findings. J Breast Cancer. 2012;15(2):258–260. https://doi.org/10.4048/jbc.2012.15.2.258

Buck AK, Schirrmeister H, Mattfeldt T, Reske SN. Biological characterisation of breast cancer by means of PET. Eur J Nucl Med Mol Imaging. 2004;31 Suppl 1:S80–S87. https://doi.org/10.1007/s00259-004-1529-6

Carlsen J, Ewertsen C, Sletting S et al. Ultrasound elastography in breast cancer diagnosis. Ultraschall Med. 2015;36(06):550–565. https://doi.org/10.1055/s-0035-1553293

Chen CC, Weng HH, Hwang CE et al. Acute leukemia presenting with extramedullary diseases and completely normal hemogram: an extremely unusual manifestation unique to pre-B ALL. American J Hematol. 2010;85(9):729–731. https://doi.org/10.1002/ajh.21801

Chim CS, Shek TW, Liang R. Isolated relapse of acute lymphoblastic leukemia in the breast masquerading as gynecomastia. Am J Med. 2000;108(8):677–679. https://doi.org/10.1016/S0002-9343(99)00397-6

Cunningham I. A clinical review of breast involvement in acute leukemia. Leuk Lymphoma. 2006;47(12):2517–2526. https://doi.org/10.1080/10428190600967022

Cunningham I. Post-transplant leukemia relapse in organs: biology and behavior in 585 reports. Crit Rev Oncol/Hematol. 2021;157:103170. https://doi.org/10.1016/j.critrevonc.2020.103170

De Cap MR, Chen W. Myeloid sarcoma: an overview. Semin Diagn Pathol. 2023;40(3):129–139. https://doi.org/10.1053/j.semdp.2023.04.009

DiNardo CD, Erba HP, Freeman SD, Wei AH. Acute myeloid leukaemia. Lancet (London, England). 2023;401(10393):2073–2086. https://doi.org/10.1016/S0140-6736(23)00108-3

Durhan G, Demirkazık F. Breast involvement of hematological malignancies: imaging and clinical findings. Egypt J Radiol Nucl Med. 2021;52(1):172–178. https://doi.org/10.1186/s43055-021-00558-2

Erduran E, Gedik Y, Orhan F, Reis A. Leukemic infiltrations of the peritoneum at diagnosis and the breast at relapse in a child with acute B-cell lymphoblastic leukemia. Med Pediatr Oncol. 1999;32(1):71–72. https://doi.org/10.1002/(SICI)1096-911X(199901)32:1<71::AID-MPO18>3.0.CO;2-1

Galimberti S, Benedetti E, Morabito F et al. Different gamma/delta T clones sustain GVM and GVH effects in multiple myeloma patients after non-myeloablative transplantation. Leuk Res. 2006;30(5):529–535. https://doi.org/10.1016/j.leukres.2005.09.004

Gaudichon J, Jakobczyk H, Debaize L et al. Mechanisms of extramedullary relapse in acute lymphoblastic leukemia: reconciling biological concepts and clinical issues. Blood Rev. 2019;36:40–56. https://doi.org/10.1016/j.blre.2019.04.003

Ge L, Ye F, Mao X et al. Extramedullary relapse of acute leukemia after allogeneic hematopoietic stem cell transplantation: different characteristics between acute myelogenous leukemia and acute lymphoblastic leukemia. Biol Blood Marrow Transplant. 2014;20(7):1040–1047. https://doi.org/10.1016/j.bbmt.2014.03.030

Ghosh V, Roy S, Dhamija E et al. Extramedullary relapse of B cell acute lymphoblastic leukemia in bilateral breasts treated with whole breast radiotherapy. J Adolescent Young Adult Oncol. 2023;12(6):942–947. https://doi.org/10.1089/jayao.2022.0145

Glazebrook KN, Zingula S, Jones KN, Fazzio RT. Breast imaging findings in haematological malignancies. Insights Imaging. 2014;5(6):715–722. https://doi.org/10.1007/s13244-014-0344-2

Goker H, Haznedaroglu IC, Chao NJ. Acute graft-vs-host disease: pathobiology and management. Exp Hematol. 2001;29(3):259–277. https://doi.org/10.1016/S0301-472X(00)00677-9

Houghtelin AB, Kopp LM, Pelayo-Katsanis L et al. Extramedullary breast relapse of acute lymphoblastic leukemia controlled with a second allogeneic/autologous hematopoietic cell transplant. J Adolesc Young Adult Oncol. 2015;4(1):50–53. https://doi.org/10.1089/jayao.2014.0018

Hussain Y, Alsharif KF, Aschner M et al. Therapeutic role of carotenoids in blood cancer: mechanistic insights and therapeutic potential. Nutrients. 2022;14(9):1949. https://doi.org/10.3390/nu14091949

Karbasian-Esfahani M, Wiernik PH, Yeddu M, Abebe L. Leukemic infiltration of the breast in acute lymphocytic leukemia (ALL). Hematology (Amsterdam, Netherlands). 2008;13(2):101–106. https://doi.org/10.1179/102453308X315933

Khoury NJ, Al-Kass FMH, Jaafar HN, Taher AT, Shamseddine AI. Bilateral breast involvement in acute myelogenous leukemia. Eur Radiol. 2000;10(6):1031. https://doi.org/10.1007/s003300051059

Kim SJ, Kim WG. Sonographic features of a myeloid sarcoma of the breast as a relapse of acute myeloid leukemia after stem-cell transplantation: a case report. Am J Case Rep. 2019;20:612–619. https://doi.org/10.12659/AJCR.915453

Kim SJ. Magnetic resonance imaging features of breast leukemia. Magn Reson Med Sci. 2013;12(4):309–313. https://doi.org/10.2463/mrms.2012-0091

Koh DM, Collins DJ. Diffusion-weighted MRI in the body: applications and challenges in oncology. Am J Roentgenol. 2007;188(6):1622–1635. https://doi.org/10.2214/AJR.06.1403

Kulkarni RS, Anand AS, Parikh SK, Patel P. Pre-B acute lymphoblastic leukemia masquerading as breast carcinoma: a rare case report. Clin Cancer Investig J. 2016;5(6):544–547. https://doi.org/10.4103/2278-0513.200112

Kumar PR, Grossman Z, Scorza L, Khoury T, Nayyar R. Isolated extramedullary relapse of acute lymphoblastic leukemia in the breast of an adolescent girl: radiologic findings and discussion. Pediatr Radiol. 2010;40(5):773–776. https://doi.org/10.1007/s00247-009-1485-1

Lee JH, Choi SJ, Lee JH et al. Anti-leukemic effect of graft-versus-host disease on bone marrow and extramedullary relapses in acute leukemia. Haematologica. 2005;90:1380–1388. https://pubmed.ncbi.nlm.nih.gov/16219575/

Lee NR, Oh HK, Jeong YJ. Clinical significance of ultrasound elastography and fibrotic focus and their association in breast cancer. J Clin Med. 2022;11(24):7435. https://doi.org/10.3390/jcm11247435

Li J, Sun B, Li Y et al. Correlation analysis between shear-wave elastography and pathological profiles in breast cancer. Breast Cancer Res Treat. 2023;197(2):269–276. https://doi.org/10.1007/s10549-022-06804-z

Likaki-Karatza E, Mpadra FA, Karamouzis MV et al. Acute lymphoblastic leukemia relapse in the breast diagnosed with gray-scale and color Doppler sonography. J Clin Ultrasound. 2002;30(9):552–556. https://doi.org/10.1002/jcu.10118

Liu B, Liu B, Wang X et al. Complete response of extramedullary relapse in breast of acute T lymphoblastic leukemia after bone marrow transplantation to chemoradiotherapy: a case report and literature review. BMC Cancer. 2016;16(1):875. https://doi.org/10.1186/s12885-016-2910-0

Masood L, Sayeed S, Aslam S. Acute lymphoblastic leukemia simulating breast carcinoma. Egypt J Radiol Nucl Med. 2021;52(1):224. https://doi.org/10.1186/s43055-021-00608-9

Mosalem O, Rous FA, Elshafie A, Isaac D. Bilateral breast masses as a presentation for T-cell acute lymphoblastic leukaemia. BMJ Case Rep. 2020;13(8):e236263. https://doi.org/10.1136/bcr-2020-236263

Myers CB, Ene A, Clark A. A rare presentation of myeloid sarcoma as symmetrical bilateral breast masses. Clin Imaging. 2022;85:94–98. https://doi.org/10.1016/j.clinimag.2022.02.023

Nasief HG, Rosado-Mendez IM, Zagzebski JA, Hall TJ. A quantitative ultrasound-based multi-parameter classifier for breast masses. Ultrasound Med Biol. 2019;45(7):1603–1616. https://doi.org/10.1016/j.ultrasmedbio.2019.02.025

Pagliuca S, Gurnari C, Hercus C et al. Leukemia relapse via genetic immune escape after allogeneic hematopoietic cell transplantation. Nat Commun. 2023;14(1):3153. https://doi.org/10.1038/s41467-023-38113-4

Sager O, Dincoglan F, Demiral S et al. Breathing adapted radiation therapy for leukemia relapse in the breast: a case report. World J Clin Oncol. 2019;10(11):369–374. https://doi.org/10.5306/wjco.v10.i11.369

Shatilova A, Girshova L, Zaytsev D et al. The myeloid sarcoma treated by Venetoclax with hypomethylating agent followed by stem cell transplantation: rare case report. BMC Women's Health. 2021;21(1):184. https://doi.org/10.1186/s12905-021-01328-y

Shin HC. Relapse of biphenotypic acute leukemia as a breast mass. J Breast Cancer. 2016;19(4):455–458. https://doi.org/10.4048/jbc.2016.19.4.455

Sosa YJ, Pope D, Monetto FEP, Robinson A, Klimberg VS. Hematologic malignancies of the breast: report of three cases. Radiol Case Rep. 2022;17(5):1384–1390. https://doi.org/10.1016/j.radcr.2022.02.004

Spak DA, Plaxco JS, Santiago L, Dryden MJ, Dogan BE. BI-RADS(®) fifth edition: a summary of changes. Diagn Interv Imaging. 2017;98(3):179–190. https://doi.org/10.1016/j.diii.2017.01.001

Sung P, Lee JY, Chu AJ. Relapsed acute myeloid leukemia presenting as multiple breast masses: a case report. J Korean Soc Radiol. 2023;84(2):454–459. https://doi.org/10.3348/jksr.2022.0062

Surov A, Wienke A, Abbas J. Breast leukemia: an update. Acta Radiol. 2012;53(3):261–266. https://doi.org/10.1258/ar.2011.110470

Surov A. Imaging findings of hematologic diseases affecting the breast. Semin Ultrasound, CT, MR. 2013;34(6):550–557. https://doi.org/10.1053/j.sult.2013.05.001

Waks AG, Winer EP. Breast cancer treatment: a review. JAMA. 2019;321(3):288–300. https://doi.org/10.1001/jama.2018.19323

Yang WT, Lane DL, Le-Petross HT, Abruzzo LV, Macapinlac HA. Breast lymphoma: imaging findings of 32 tumors in 27 patients. Radiology. 2007;245(3):692–702. https://doi.org/10.1148/radiol.2452061726

Zhang H, Hu Y, Wei G, Wu W, Huang H. Successful chimeric antigen receptor T cells therapy in extramedullary relapses of acute lymphoblastic leukemia after allogeneic hematopoietic stem cell transplantation. Bone Marrow Transplant. 2020;55(7):1476–1478. https://doi.org/10.1038/s41409-019-0778-8